



**HAL**  
open science

## Racemic compound and conglomerate of anhydrous sibutramine hydrochloride: a rare case of relative stability

F Rosa, P Négrier, P Espeau

► **To cite this version:**

F Rosa, P Négrier, P Espeau. Racemic compound and conglomerate of anhydrous sibutramine hydrochloride: a rare case of relative stability. CrystEngComm, 2016, 18 (36), pp.6903 - 6907. 10.1039/C6CE01123C . hal-01392663

**HAL Id: hal-01392663**

**<https://hal.science/hal-01392663>**

Submitted on 4 Nov 2016

**HAL** is a multi-disciplinary open access archive for the deposit and dissemination of scientific research documents, whether they are published or not. The documents may come from teaching and research institutions in France or abroad, or from public or private research centers.

L'archive ouverte pluridisciplinaire **HAL**, est destinée au dépôt et à la diffusion de documents scientifiques de niveau recherche, publiés ou non, émanant des établissements d'enseignement et de recherche français ou étrangers, des laboratoires publics ou privés.



Distributed under a Creative Commons Attribution - ShareAlike 4.0 International License

# Racemic compound and conglomerate of anhydrous sibutramine hydrochloride: a rare case of relative stability†

F. Rosa,<sup>a</sup> P. Négrier<sup>b</sup> and P. Espeau<sup>\*a</sup>

The thermal behaviours of racemic sibutramine hydrochloride monohydrate as well as that of the anhydrous state were investigated by DSC. A new anhydrous solid was then put in evidence and its crystal structure was solved from XRPD data. This new phase was found to be the conglomerate. Depending on the heat treatment, the initial anhydrous racemic compound may be completely resolved. DSC analyses have shown that the anhydrous conglomerate melts at a higher temperature than the anhydrous racemic compound.

## Introduction

Sibutramine hydrochloride monohydrate, *N*-(1-(4-chloro phenyl cyclobutyl)-3-methylbutyl)-*N,N*-dimethyl amine hydrochloride monohydrate, is an active substance used for the treatment of obesity. Indeed, a decrease in appetite and a satiety effect have been observed.<sup>1</sup> Nevertheless, secondary effects such as cardiovascular risk, fibrosis, a decline in fertility or serious adverse effects on the thyroid gland and liver functions have been reported.<sup>2-5</sup> In 2010, in view of the risks to patients, the European Medicines Agency decided to prohibit the marketing of this product in Europe. As a consequence, the number of counterfeit products containing sibutramine hydrochloride monohydrate has been steadily increasing.

Sibutramine hydrochloride monohydrate (*rac*-Sibut-HCl·H<sub>2</sub>O) is a crystalline racemic compound the chirality of which is due to the presence of a sp<sup>3</sup>-hybridized carbon with four different moieties, including a secondary amine group (Scheme 1). Hence, two enantiomers, the *R*-configuration and the *S*-configuration, as well as the equimolar mixture between the two enantiomers, are encountered. The racemic compound is the only product commercially available.

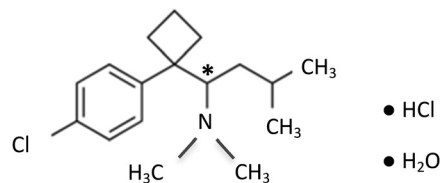
Upon heating, *rac*-Sibut-HCl·H<sub>2</sub>O dehydrates at around 100 °C.<sup>6-10</sup> The melting temperatures of the so-obtained racemic anhydrous compound vary, according to the authors, from 188 to 197 °C, with melting enthalpies ranging from 91 to 97 J g<sup>-1</sup>. The crystal structure of the anhydrous phase, obtained from single crystal X-ray diffraction, was also reported in the literature.<sup>10</sup>

The present study focuses on the anhydrous state of sibutramine hydrochloride. We show that, starting from the commercial hydrated form, the anhydrous solid state of S-HCl may exhibit two different phases, depending both on the heating rates applied by differential scanning calorimetry and the annealing conditions. These two phases are then characterised combining differential scanning calorimetry (DSC), thermogravimetric analysis (TGA) and X-ray powder diffraction (XRPD). Then, a thermodynamic relationship between those two anhydrous crystalline forms is proposed, based on the binary phase diagram involving the two enantiomers *R* and *S*.

## Experimental

### Chemicals

Sibutramine hydrochloride monohydrate (*rac*-Sibut-HCl·H<sub>2</sub>O) was purchased from Molekula, with purity higher than 98%. The compound was used without further purification.



**Scheme 1** Molecular structure of sibutramine hydrochloride monohydrate (\*: asymmetric carbon).

<sup>a</sup> Unité de Technologies Chimiques et Biologiques pour la Santé, Inserm U 1022 CNRS UMR 8258, Faculté des Sciences Pharmaceutiques et Biologiques, Université Paris Descartes, Sorbonne Paris Cité, 4 avenue de l'Observatoire, 75006 Paris, France. E mail: philippe.espeau@parisdescartes.fr

<sup>b</sup> Laboratoire Ondes et Matière d'Aquitaine, UMR CNRS 5798, Université de Bordeaux, 351 cours de la Libération, 33405 Talence Cedex, France

## X-ray powder diffraction

XRPD experiments were performed with a horizontally mounted cylindrical position-sensitive detector CPS-120 (Debye–Scherrer geometry, transmission mode) from INEL, using monochromatic Cu  $K\alpha_1$  radiation ( $\lambda = 1.5406 \text{ \AA}$ ), selected with an asymmetric focusing incident-beam curved quartz monochromator. The generator power was set to 1.0 kW (40 kV and 25 mA). The detector consisted of 4096 channels providing angular step of  $0.029^\circ$  (2) between  $4^\circ$  and  $120^\circ$ . External calibration using the  $\text{Na}_2\text{Ca}_2\text{Al}_2\text{F}_{14}$  (NAC) cubic phase mixed with silver behenate was performed by means of cubic spline fittings. From that, each channel was converted into a diffraction angle.

The samples were gently crushed before being introduced into Lindemann glass capillaries with 0.5 mm inner diameter, which were then rotated perpendicular to the X-ray beam direction in order to decrease as much as possible the effects of preferred orientations.

Crystal structure was determined with the reflex plus module of Materials Studio Modeling 5.5.<sup>11</sup> First, the pattern was indexed by means of the peak picking option of the software package. Potential solutions for cell parameters and space group were found using the X-cell algorithm.<sup>12</sup> Then, a Pawley profile-fitting procedure<sup>13</sup> was applied, including refined cell parameters, experimental profile fitting with pseudo-Voigt function and zero shift. Distances, angles and torsions in the molecule were obtained *via* energy-minimization calculations with the forcite module using the Dreiding force field.<sup>14</sup> Then, a Monte-Carlo approach, included in the reflex plus module, was carried out in the direct space to solve the structure moving the molecule as a rigid-body and allow the change of the chain torsion angles.<sup>15</sup> The structure refinement was achieved using the Rietveld method combined with energy minimization, including Pawley refined parameters, rigid-body molecular units, torsions, overall isotropic factor and March–Dollase preferred orientations.<sup>16</sup>

## Thermal analysis

Differential scanning calorimetry and thermo-gravimetric analysis experiments were performed using an 822e thermal analyser, equipped with an FRS5 sensor, and a TGA 850 from Mettler-Toledo (Switzerland). The DSC and TGA experiments were carried out in the 25 to 250 °C temperature range, at different scan rates from 1 to 20 °C min<sup>-1</sup> and under a constant nitrogen flow. Temperature and enthalpy calibration of the apparatus were carried out at 10 °C min<sup>-1</sup>. Indium and zinc were used for temperature and enthalpy calibration. Regarding the enthalpy values, a relative standard uncertainty on the values was estimated at 5%. For all the experiments, an empty aluminium pan was used as a reference. The melting temperatures were determined at the onset of the corresponding endotherms. Samples were weighed with a microbalance sensitive to 1 µg and then introduced into a crucible with a perforated cover. The standard uncertainty on the temperatures was determined from the standard deviation of three independent measurements.

## Results and discussion

The XRPD pattern of the starting material, *i.e.* the commercial product *rac*-Sibut-HCl·H<sub>2</sub>O, was recorded at room temperature and was found to be the same as the profile calculated from the crystal structure.<sup>17</sup> The Pawley refinement and the comparison of the unit cell parameters can be found as part of the ESI† (Table S1 and Fig. S1).

Then, a first thermal characterisation of *rac*-Sibut-HCl·H<sub>2</sub>O was carried out by DSC and TGA at 5 °C min<sup>-1</sup>. The DSC curve (Fig. 1) reveals a first endothermic peak at ~100 °C, corresponding to the dehydration of the compound. A weight loss of approximately 5.5% was determined by TGA (Fig. 1), which corresponds to the loss of one molecule of water. The enthalpy of dehydration was found to be  $41.2 \pm 2.8 \text{ kJ}$  per mole of water, comparable to previously reported values for similar molecules presenting internal cavities: 45.5 kJ per mole of water for quinacrine dihydrochloride hydrate<sup>18</sup> and between 50 and 63 kJ per mole of water for  $\beta$ -cyclodextrin hydrates<sup>19</sup> and hydrated cucurbituril.<sup>20</sup>

Still on heating after dehydration, two endothermic peaks were then observed, approximately at 194 °C and 205 °C. This result disagrees with previous DSC analyses,<sup>6–10</sup> in which only one endothermic peak was observed for the melting of the anhydrous phase, at a temperature comprised between 188 and 197 °C.

As can be seen on the zoom of Fig. 1, the first endothermic peak at 194 °C was followed by a recrystallization process. This suggests that this first endothermic peak has to be associated to a melting process. Then, still on heating, the second endothermic peak appears at 205 °C, and should correspond to the melting point of another solid phase. The TGA curve (Fig. 1) revealed a weight loss of approximately 4% just before and during melting, *i.e.* during the melting–crystallization–melting sequence. This weight loss could be explained as sublimation and evaporation of the sample. This was confirmed from experiments carried out at high scan rates, up to 100 °C min<sup>-1</sup> (results not shown), where no more mass loss was then observed. Moreover, this phenomenon could not be attributed to degradation since the onset of the first endothermic signal did not vary

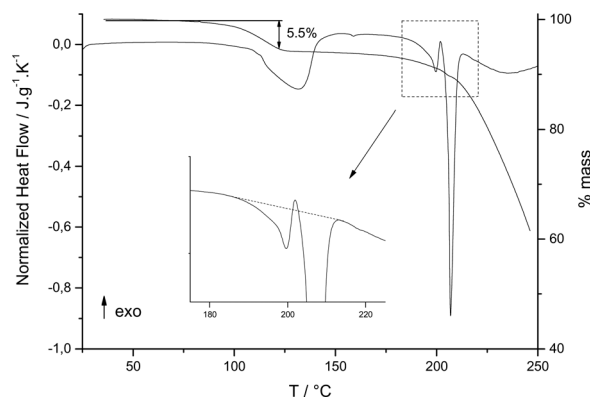


Fig. 1 DSC and TGA curves of *rac*-Sibut-HCl·H<sub>2</sub>O recorded at 5 °C min<sup>-1</sup>. The inset corresponds to the zoom of the melting region between 190 and 220 °C, showing the melting–crystallization–melting sequence.

with the heating rate. When degradation occurs upon melting, it is well known that the “apparent” melting temperature increases with the DSC heating rate.<sup>21</sup>

After melting, one can observe on the DSC and TGA curves (Fig. 1) that the molten anhydrous sibutramine (Sibut·HCl) degrades. Indeed, the broad DSC endothermic peak following melting is accompanied with an important weight loss.

Depending on the heating rate, the relative intensities of both melting peaks changed (Fig. 2). More precisely, when increasing the heating rate, the intensity of the second peak increased compared to the first one. This suggests that each peak may correspond to the melting of one different anhydrous form of Sibut·HCl.

To confirm this assumption and to be able to characterise each anhydrous solid, different methods of preparation were used to try and isolate each form.

First, the commercial product was dehydrated at 120 °C and the so-obtained anhydrous compound was annealed for several days at this temperature. After that, a DSC experiment was performed on heating of the annealed solid and a single endothermic peak was observed at  $198.8 \pm 0.2$  °C (curve 1 in Fig. 3), with an associated melting enthalpy of  $38.8 \pm 1.6$  kJ mol<sup>-1</sup>. The same behaviour was observed when *rac*-Sibut·HCl·H<sub>2</sub>O was ground before introducing it into the DSC pan (curve 2 in Fig. 3).

Interestingly, when dehydrated sibutramine hydrochloride was recrystallised in anhydrous methanol, and rehydrated in ambient conditions, a single melting peak was also observed by DSC but, this time, at a higher temperature equal to  $205.0 \pm 0.3$  °C, with an associated melting enthalpy of  $27.8 \pm 0.6$  kJ mol<sup>-1</sup> (curve 3 in Fig. 3). The same melting point was noticed when the anhydrous form was obtained from ground *rac*-Sibut·HCl·H<sub>2</sub>O dehydrated at 180 °C (result not shown).

These results showed that the two peaks observed in Fig. 1 were not an experimental artefact, but consistent with the existence of two distinct anhydrous phases. To confirm this finding, the two solids obtained by the two preceding methods were characterised by XRPD.

The pattern matching of the anhydrous form obtained by annealing at 120 °C (called in the following anhydrous A) was

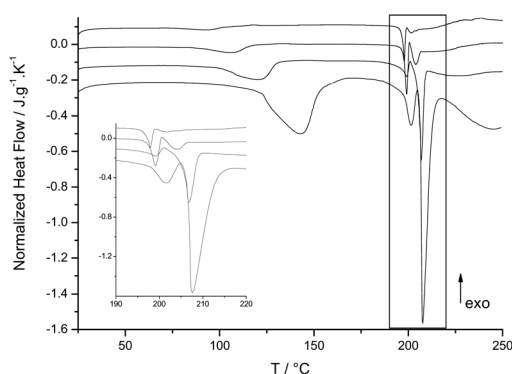


Fig. 2 Normalized DSC curves of *rac* Sibut·HCl·H<sub>2</sub>O recorded at 1, 2, 5 and 20 °C min<sup>-1</sup> (from top to bottom). The inset corresponds to the zoom of the melting region between 190 and 220 °C.

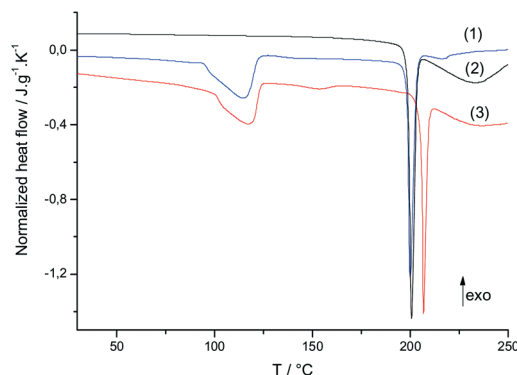


Fig. 3 Normalized DSC curves recorded at 10 °C min<sup>-1</sup> of *rac* Sibut·HCl·H<sub>2</sub>O and Sibut·HCl. (1) Anhydrous solid annealed at 120 °C, (2) ground *rac* Sibut·HCl·H<sub>2</sub>O, (3) recrystallised anhydrous solid rehydrated in ambient conditions.

determined at room temperature. The space group and cell parameters were found to match with the previously reported crystal structure determined on single crystal obtained by sublimation/decomposition of the monohydrate form at 190 °C.<sup>10</sup> The Pawley refinement and the unit cell parameters are given in Fig. S2 and Table S2† respectively. The structure showed that the anhydrous compound is a racemic compound with a unit cell consisting of two molecules having the *R* configuration and two having the *S* configuration.

The unknown crystal structure of the anhydrous form whose melting point was found at 205 °C (called anhydrous B in the following) was determined from an XRPD pattern recorded at room temperature during eight hours. The diffraction pattern was reproduced with a monoclinic space group *P*2<sub>1</sub> and with cell parameters: *a* = 12.0282(19) Å, *b* = 9.0364(15) Å, *c* = 8.1578(11) Å,  $\beta$  = 90.601(9)°. The final Rietveld refinement (Table S3†) converged to a final *R*<sub>wp</sub> value of 4.36% (Fig. 4).

The crystal structure reveals that only one enantiomer is present in the unit cell, as shown in Fig. 5. This indicates that the initial anhydrous racemic compound (anhydrous A) was transformed into conglomerate. This explains why one

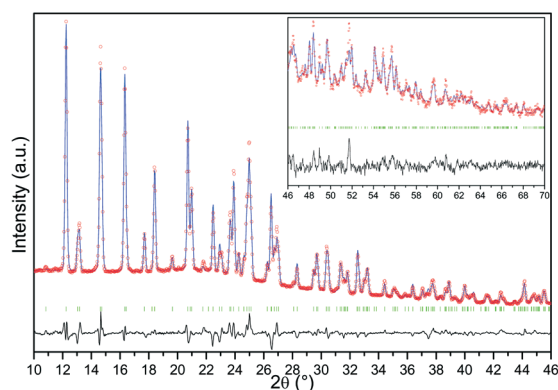


Fig. 4 Final Rietveld refinement of X ray diffraction pattern of sibutramine obtained at 294 K (anhydrous B). Blue line: Experimental pattern, empty red circles: calculated pattern, green vertical bars: peak positions, black line: residual XRPD patterns. The inset corresponds to the scale for the data between 46° and 70° magnified 15 times.

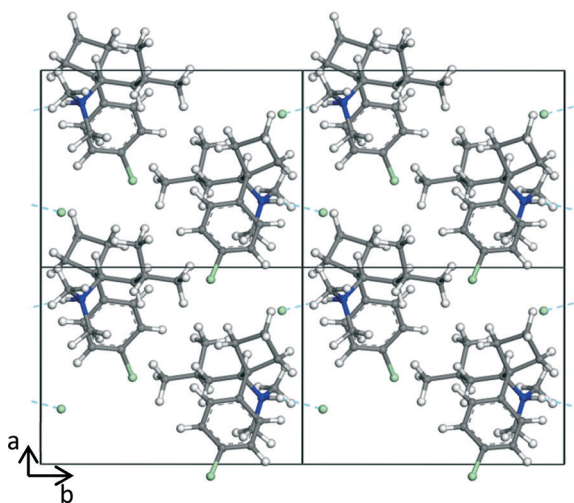


Fig. 5 Crystal structure of anhydrous sibutramine B viewed along *c*.

parameter, in this case *b*, is divided approximately by 2 compared to anhydrous A, formed by an alternating stack of *R*- and *S*-enantiomers. However, both structures have nearly the same density in the solid state: 1.185 g cm<sup>-3</sup> for the conglomerate instead of 1.180 g cm<sup>-3</sup> for the racemic compound.<sup>10</sup>

The structure is maintained by seven inter-molecular H-bonds mainly between the secondary amine group and the counter ion Cl2 (Table 1). The other chlorine atom Cl1, coming from the chlorobenzene group, also initiates H-bond interactions with C6 and C12. However these interactions remain weaker (Table 1).

By comparison, six H-bonds were reported for anhydrous A (Table S4<sup>†</sup>). As for anhydrous B, *S*-HCl interacts with Cl2 through an H-bond interaction with N1 but also with C10 and C11. The distances and the angles are almost identical in both structures. The C17 methyl group interacts with Cl1, while it interacts with Cl2 in anhydrous B. This is explained by the fact that the methyl groups are not positioned in the same manner in both anhydrous, as discussed below.

As observed in Fig. 6 and reported in Table 2, the conformation differences between the molecules of A and B are mainly noticeable for the isobutyl group. As can be seen in Table 2 and Fig. 6-1, the C16 and C17 methyl groups rotated of about 107° and C15 by 78.4°.

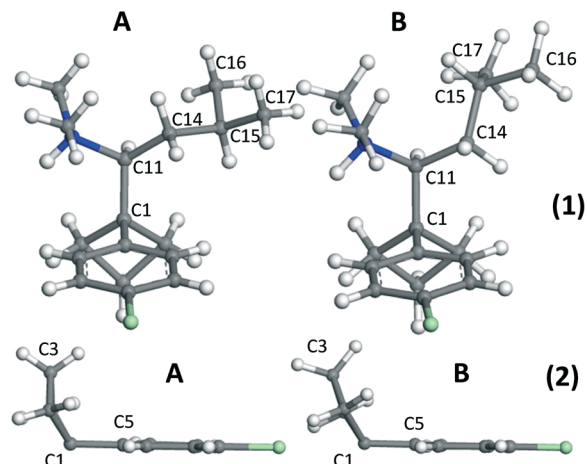


Fig. 6 Molecular conformations of the anhydrous A and B of sibutramine. (1) Part of the molecule including the secondary amine and isobutyl groups. (2) part of the molecule including the phenyl and cyclobutane groups.

The cyclobutane group was found to be less planar in anhydrous A than in anhydrous B (Fig. 6-2), as stated by the angle between C2–C3–C4 and C1–C2–C4 planes which equals 13.8° for anhydrous B and 30.3° for A, as well as the angle between C1–C2–C3 and C1–C3–C4 planes equal to 14.6° for anhydrous B and 30.4° for A.

Regarding the phenyl group, it has practically undergone no major changes (Fig. 6-2, Table 2) and remained almost planar in both conformations.

Taking these new findings into account, the endothermic peak observed in the DSC curve 3 in Fig. 3 at 139.6 ± 3.6 °C, with an associated heat of 2.6 ± 1.0 kJ mol<sup>-1</sup>, can be ascribed to a peritectoid transformation of the anhydrous racemic compound into conglomerate.<sup>22</sup> Above this point, the conglomerate becomes more stable than the racemic compound. This explains why the conglomerate (in a stable state) melts at a higher temperature than the racemic compound (in a metastable state), *i.e.* 205 °C instead of 198.8 °C. From an energetic point of view, the conglomerate melts with a lower enthalpy than the racemic compound (27.8 instead of 38.8 kJ mol<sup>-1</sup>). Such behaviour has been previously reported for racemic 1,1'-binaphthyl<sup>23</sup> or for hydantoin derivative.<sup>24</sup>

The anhydrous racemic compound is always obtained after dehydration of *rac*-Sibut·HCl·H<sub>2</sub>O whatever the

Table 1 Inter molecular H bond distances and angles for anhydrous B

D	H	A	D H (Å)	H···A (Å)	D···A (Å)	D H···A (deg.)	Symmetry
N1	H1	Cl2	1.041(5)	2.098(7)	3.060(7)	152.6(5)	i
C10	H10	Cl2	1.025(5)	2.803(7)	3.749(7)	153.5(4)	i
C11	H11	Cl2	1.098(9)	2.763(8)	3.800(8)	157.4(4)	ii
C13	H13A	Cl2	1.099(11)	2.610(9)	3.593(9)	148.5(4)	ii
C17	H17C	Cl2	1.088(8)	2.93(6)	3.885(9)	146.9(5)	v
C12	H12B	Cl1	1.092(11)	2.91(8)	3.852(6)	144.9(6)	iii
C6	H6	Cl1	1.018(7)	2.97(7)	3.854(8)	145.8(7)	iv

(i)  $-x, 1/2 + y, 1 - z$ ; (ii)  $x, 1 + y, z$ ; (iii)  $x, y, z + 1$ ; (iv)  $1 - x, 1/2 + y, -z$ ; (v)  $x, 1 + y, z$ .

**Table 2** Torsion angles for anhydrous forms of sibutramine

Torsion angles	Anhydrous A	Anhydrous B
C1 C11 C14 C15	82.6	161.0
C11 C14 C15 C16	72.0	-178.9
C11 C14 C15 C17	-165.7	-58.3
C5 C1 C11 C14	55.4	62.7
C5 C1 C11 N1	-72.9	-68.9
C5 C1 C2 C3	-91.6	-103.1
C12 N1 C11 C14	38.6	-37.8
C13 N1 C11 C14	-86.1	93.4

experimental conditions. However, no analogy was found between the crystal structures of *rac*-Sibut-HCl·H<sub>2</sub>O and *rac*-Sibut-HCl (Fig. S3†). Indeed, the molecular arrangements seen in two different directions do not show any possible structural filiation between both structures.<sup>25</sup> Then, one can assume that the hydrated material undergoes a destructive process when the water molecules are released followed by a reconstructive process since the resulting phase is the anhydrous crystalline racemic phase *rac*-Sibut-HCl.

## Conclusion

By coupling thermal analyses and XRPD experiments, it was shown that, depending on experimental conditions, the dehydration of *rac*-Sibut-HCl·H<sub>2</sub>O led to either the anhydrous racemic form or the conglomerate. When the racemic compound is stabilized, it transformed into conglomerate through a peritectoid reaction that occurs at around 140 °C. Then, it was shown by DSC that the anhydrous conglomerate melts at higher temperatures than the racemic compound. When the racemic compound persists above this point, it becomes metastable and its melting point necessarily takes place before that of the stable conglomerate, but with a higher melting enthalpy.

## Acknowledgements

This work was financially supported by the ANR project "AlyPOTEC". Ms. K. Debbasch is kindly thanked for her advice on the manuscript.

## References

- 1 S. Higgs, A. J. Cooper and N. M. Barnes, *Psychopharmacology*, 2011, 214, 941.
- 2 Y. H. Zhou, X.-Q. Ma, C. Wu, J. Lu, S.-S. Zhang, J. Guo, S.-Q. Wu, X.-F. Ye, J.-F. Xu and J. He, *PLoS One*, 2012, 7, e39062.
- 3 H. M. Oberholzer, C. van der Schoor and M. J. Bester, *Environ. Toxicol. Pharmacol.*, 2015, 40, 71.
- 4 A. Saleh Bin Bisher, *Indian J. Sci. Technol.*, 2010, 3, 1129.
- 5 C. S. Borges, G. Missassi, E. S. A. Pacini, L. Ri, A. Kiguti, M. Sanabria, R. F. Silva, T. P. Banzato, J. E. Perobelli, A. S. Pupo and W. G. Kempinas, *PLoS One*, 2013, 8, e66091.
- 6 I. Nicolás-Vázquez, J. Hinojosa Torres, J. Cruz Borbolla, R. Miranda Ruvalcaba and J. M. Aceves-Hernández, *J. Mol. Struct.*, 2014, 1062, 1.
- 7 A. Ravikiran, M. Arthanareeswari, P. Kamaraj, C. Praveen and K. V. Pavan, *Chem. Sci. Trans.*, 2013, 2, S288.
- 8 P. R. Oliveira, H. K. Stulzer, L. S. Bernardi, S. H. M. Borgmann, S. G. Cardoso and M. A. S. Silva, *J. Therm. Anal. Calorim.*, 2010, 100, 277.
- 9 A. Pajzderska, D. M. Chudoba, J. Mielcarek and J. Wasicki, *J. Pharm. Sci.*, 2012, 101, 3799.
- 10 E. Maccaroni, E. Alberti, L. Malpezzi, N. Masciocchi and C. Pellegatta, *J. Pharm. Sci.*, 2008, 97, 5229.
- 11 *Materials Studio Modeling 5.5.*, (<http://accelrys.com/products/collaborative-science/biovia-materials-studio/>).
- 12 M. A. Neumann, *J. Appl. Crystallogr.*, 2003, 36, 356.
- 13 G. S. Pawley, *J. Appl. Crystallogr.*, 1981, 14, 357.
- 14 S. L. Mayo, B. D. Olafson and W. A. Goddard III, *J. Phys. Chem.*, 1990, 94, 8897.
- 15 G. E. Engel, S. Wilke, O. König, K. D. M. Harris and F. J. J. Leusen, *J. Appl. Crystallogr.*, 1999, 32, 1169.
- 16 W. A. Dollase, *J. Appl. Crystallogr.*, 1986, 19, 267.
- 17 Y. Chen, H. W. Zhou and J. Z. Chen, *Z. Kristallogr.*, 2005, 220, 513.
- 18 R. Rotival, P. Espeau, Y. Corvis, F. Guyon and B. Do, *J. Pharm. Sci.*, 2011, 100, 3223.
- 19 M. Bilal, C. de Brauer, P. Claudy, P. Germain and J. M. Létouffé, *Thermochim. Acta*, 1995, 249, 63.
- 20 P. Germain, J. M. Létouffé, M. P. Merlin and H. J. Buschmann, *Thermochim. Acta*, 1998, 315, 87.
- 21 Y. Corvis, M.-C. Menet, P. Négrier, M. Lazerges and P. Espeau, *New J. Chem.*, 2013, 37, 761.
- 22 G. Coquerel, *Enantiomer*, 2000, 5, 481-498.
- 23 K. R. Wilson and R. E. Pincock, *J. Am. Chem. Soc.*, 1975, 97, 1474.
- 24 Y. Amharar, S. Petit, M. Sanselme, Y. Cartigny, M.-N. Petit and G. Coquerel, *Cryst. Growth Des.*, 2011, 11, 2453-2462.
- 25 S. Petit and G. Coquerel, *Chem. Mater.*, 1996, 8, 2247-2258.